Comparative Pharmacological and Phytochemical Evaluation of Raw and Herb-Processed Salt Formulations

Sugeevan Rakulini

Faculty of Siddha Medicine, University of Jaffna, Sri Lanka

ABSTRACT

Salt obtained from terrestrial, marine, or botanical sources possesses distinct antiperiodic, emetic, laxative, stomachic, and vermifuge properties supporting its widespread application in traditional therapies. In Siddha medicine dietary regulation (*Pathiyam*) is divided into *Itchapathiyam* and *Kadumpathiyam* is fundamental to therapeutic success, requiring strict salt restriction during and after treatment. In post-treatment protocols typically involve external applications of *omum*-cow's milk paste alongside dietary inclusion of roasted salt combined with cow's ghee and tamarind. Furthermore, traditional practitioners process salt by frying it with *Iyanku* leaves, botanically identified as *Clerodendrum inerme* and *Azima tetracantha* in the *Sampasivampillai* Dictionary. This study aimed to assess scientifically the four types of salt forms (S 1- S 4) utilized in Siddha diets, crude salt, thermally processed salt, and salt processed with *Clerodendrum inerme*, and *Azima tetracantha*. All four preparations were evaluated by scanning electron microscopy (SEM), Fourier transform infrared spectroscopy (FTIR), and high-performance thin-layer chromatography (HPTLC). Aqueous solubility was observed across all samples. Evaluation of the organoleptic properties revealed that S1 and S2 were white crystalline structures, while S3 was a pale white crystalline structure and S4 was a pale whitish-grey crystalline structure. SEM analysis demonstrated a progressive reduction in particle dimensions: S1 (64.60 -140.1 µm) S2 (33.37- 53.01 µm), S3 (43.13 - 68.76 nm), and S4 (130.6 - 419.1 nm), which may enhance bioavailability. FTIR spectra confirmed O–H stretching bands in S1, S3, and S4, whereas S2 displayed an aromatic NH2 vibration indicative of primary amines. The HPTLC six distinct peaks for S3 and eight for S4, confirming the integration of diverse plant-derived secondary metabolites during herbal processing. Complementary spectroscopic and chromatographic analyses successfully validated the structural and chemical modifications driven by traditional processing techniques. Further analyses can offer valuable insights into the specific pharmacological actions of these compounds.

Key words: *Azima tetracantha*, *Clerodendrum inerme*, Salt, Siddha medicine, Pharmacological, Phytochemical

Recommended Citation: Sugeevan Rakulini (2026). Comparative Pharmacological and Phytochemical Evaluation of Raw and Herb-Processed Salt Formulations.. *Journal of Postgraduate Institute of Indigenous Medicine,* 1(2), 11-29. Postgraduate Institute of Indigenous Medicine.

Corresponding Author: rakulini@univ.jfn.ac.lk
Orchid ID: 0000-0001-7708-6242

Introduction

Salt is an essential component of human physiology, obtained from the terrestrial deposits, seawater, or botanical sources. Although salt refers to various chemical compounds, it generally represents common table salt. In traditional Tamil nomenclature, it is recognized by distinct variants including rock salt, sea salt, and culinary salt, and is classified into natural and artificially processed forms. Natural salts are typically purified by filtration, evaporation, or boiling, whereas commercial sea salt is systematically produced through the controlled evaporation of seawater India (Pharmacopeia, 2014).

Therapeutically, salt exhibits antiperiodic, emetic, laxative, stomachic, and vermifuge properties. When administered in small and repeated doses, common salt facilitates the appetite and aids both digestion and assimilation. At large doses, it acts as an emetic, purgative, and anthelmintic effects. Traditional practitioners in Sri Lanka frequently prescribe salt to manage indigestion, intermittent fever, phthisis, hepatic disorders, oliguria, myxoedema, and dyspepsia. Furthermore, localized application of heated salt in a poultice (*Pottani*) is useful for the treatment of scrofulous glandular enlargement, swelling, and joint diseases. Salt does not dissolve in alcohol but it dissolves in water. Dissolving in tepid water produces a crucial ingredient in saline treatment for cholera, which is administered through injection. Sea baths eliminate indigestion; therefore, they may be prepared by dissolving the salt in water. Salt is essential to all living organisms and it is mixed into animal feed to kill intestinal helminths (Pharmacopeia, 2014).

Diet regulation (*Pathiyam*) is crucial in Siddha Medicine. Not following the prescribed *Pathiyam* will cause ineffectiveness of the medicine, thereby resulting in increased and aggravated disease outcomes. In contrast, strictly adhering to *Pathiyam* eliminates disease, strengthens the body, and enhances the reputation of both the physician and medicine [2]. The dietary regimen classified as either simple (*Itchapathiyam)* or rigorous (*Kadumpathiyam*). It is determined by multifactorial parameters, including patient vitality, disease pathogenesis, medicinal potency, seasonal timing, and climatic factors (Komsta. L, 2013).

In clinical Siddha practice, *Itchapathiyam* and *Kadumpathiyam* has specified rules and regulations for consuming medicines. *Itchapathiyam*, strictly avoid

consuming specific vegetables bitter gourd, mango, brinjal, cluster beans, ash pumpkin, and sesbania. In contrast, *Kadumpathiyam* is universally enforced for regimens involving mercury-based formulations. During this rigorous phase salt should be completely restricted throughout the treatment period and for an equivalent duration post-therapy. Following this restriction, patients undergo a restorative regimen involving an external application of an *omum* (*Trachyspermum roxburghianum*) and cow's milk paste to the head and body, after which thermally processed salt may be gradually reintroduced into the diet. After three days, a subsequential bath using cow's ghee is indicated. Followed by the dietary reintroduction of tamarind (*Tamarindus indica*) (Komsta. L, 2013). Traditional protocols involve frying salt with *Iyanku* leaves, which are botanically identified as *Clerodendrum inerme* and *Azima tetracantha* in the *Sampasivampillai* dictionary (Muthaliyar, 1936; PLIM, n.d). Therefore, this study aimed to scientifically evaluate and compare the physicochemical and phytochemical profiles of four distinct ancestral salt preparations: crude salt, fried salt, and salt processed with *Clerodendrum inerme* and *Azima tetracantha*.

Objectives

The objective of this study was to provide a comprehensive scientific validation and comparative characterization of traditional salt preparations utilized in ancestral Siddha dietary practices (*Pathiyam*). To achieve this, four distinct salt formulations were systematically prepared in strict accordance with traditional protocols. The macro-properties, including appearance, crystalline structure, and aqueous solubility, were subsequently evaluated and compared across all cohorts to map their fundamental organoleptic and physicochemical profiles.

The study further aimed to characterize the microstructural features of each formulation using SEM, elucidate their functional group composition and bonding environments through FTIR, and assess the phytochemical fingerprint of the herb-fried preparations using HPTLC, to establish a scientific framework correlating traditional processing methods with their resultant physicochemical and phytochemical characteristics.

Materials and methods

Sample preparation

Four salt-based samples were prepared for analysis as described in Table 1. Commercial table salt was used as the control sample (S1).

Fried salt (S2) was prepared by heating raw salt in a clean metal pan under controlled temperature conditions until frying was complete. For the herbal salt preparations, raw salt was mixed separately with fresh *Clerodendrum inerme* leaves (S3) and fresh *Azima Tetracantha* leaves (S4) according to the traditional preparation method and heated until frying was completed. The resulting preparations were cooled to room temperature and stored in airtight containers until analysis. All samples were appropriately labeled and maintained under identical storage conditions throughout the study.

Table 1: Sample prepared for analysis

Sample	Name of the sample	Preparation method
S1	Table salt	Raw salt was purchased in retail sale shop and used without any processing
S2	Fried salt sample	Raw salt was heated in a clean metal pan under controlled temperature until the frying process was completed. The fried salt was allowed to cool to room temperature and then stored in an airtight container until further use.
S3	Salt fried with *Clerodendrum inerme*	Raw salt was mixed with fresh *Clerodendrum inerme* leaves and heated in pan until frying was completed. The resulting preparation was then cooled to room temperature and stored in an airtight container.
S4	Salt fried with *Azima Tetracantha*	Raw salt was mixed with fresh *Azima Tetracantha* leaves according to the traditional preparation method and heated in a pan until the frying process was completed. The resulting preparation was cooled to room temperature and stored in an airtight container.

The physicochemical properties of all samples (S1–S4) were evaluated by determining the percentage loss on drying, total ash, acid-insoluble ash, alcohol-soluble extractive, and water-soluble extractive values. In addition, structural and chemical characterization of the samples SEM, FTIR, HPTLC.

Physiochemical Characterization

Loss on Drying

The loss on drying was determined by accurately weighing the test drug in a pre-tared evaporating dish and drying at 105°C for 5 hours. The percentage loss was calculated relative to the initial weight of the sample (Pillai, 1994; Vagupu, 2006).

Total Ash Content

The accurately weighed quantity of the test drug was placed in a silica crucible and incinerated in a muffle furnace at 400°C until complete combustion was achieved, as indicated by the absence of carbonaceous residue and the formation of a white ash. The total ash content was expressed as a percentage of the air-dried drug weight. (Pillai, 1994; Vagupu, 2006).

Acid- Insoluble Ash

The total ash obtained form total ash content was transferred to a beaker and boiled with dilute HCl (25 mL) for 6 minutes. The acid-insoluble residue was collected by filtration using a sintered crucible, washed thoroughly with hot distilled water, and ignited to a constant weight. The acid-insoluble ash was calculated as a percentage based on the weight of air-dried ash (Pillai, 1994; Vagupu, 2006).

Alcohol - Soluble Extractive Value

The test sample was macerated with alcohol (100 mL) in a stoppered conical flask for 24 h, shaken frequently for the first 6 h, and followed by undisturbed standing for the remaining 18 hours. The mixture was rapidly filtered to minimize solvent evaporation, and 25 mL of the filtrate was transferred to a pre-tared, flat-bottomed evaporating dish. The solvent was evaporated to dryness, and the residue was dried at 105°C to a constant weight. The alcohol-soluble extractive value was expressed as a percentage of the air-dried drug (Pillai, 1994; Vagupu, 2006).

Water-Soluble Extractive Value

The test sample was macerated with 100 mL of chloroform water in a stoppered conical flask for 24 h, shaken frequently for the first 6 h, and allowed to stand for 18 h. The filtrate was rapidly filtered to minimize solvent evaporation, and 25 mL of the filtrate was evaporated to dryness in a tared, flat-bottomed, shallow dish. The residue was dried at 105 ºC to a constant weight, and weighed. The percentage of water-soluble extracts was calculated based on the air-dried drug (Pillai, 1994; Vagupu, 2006).

SEM

The surface morphology and particle size of the test sample were examined using scanning electron microscopy (FEI Quanta 200 FEG; Berlin, Germany). Prior to analysis, the powdered sample was mounted on aluminum stubs and sputter-coated with gold to enhance conductivity and image resolution. Morphology characterization was performed at a magnification of 100,000 x and particle size analysis at 200,000 x.

FTIR

The sample was processed using a Bruker Alpha-E spectrometer with an attenuated total reflectance (ATR) module. The sample was positioned on the crystal platform with the anvil in an upright position to ensure proper contact with the crystal before the infrared (IR) radiation exposure. The spectra were recorded over the desired wavelength, and the resulting peaks/waves were recorded for further interpretation. OPUS version 7 was used for the functional group analysis. OPUS software (Version 7). Spectral detection was carried out using a deuterated triglycine sulfate (DTGS) detector.

Chromatographic Analysis

TLC

TLC was performed samples were subjected to thin-layer chromatography (TLC) following the conventional one-dimensional ascending method using silica gel 60F254. A 7X6 cm (Merck). Plates were cut to size and sample application positions were marked using a soft pencil. Sample solutions (10 µL per track) were applied at a distance of 1 cm from the base across five tracks using a calibrated micropipette. Development was carried out in a twin-trough chamber using the specified solvent system. Following development, plates were dried and examined under visible light, short-wave UV light (254 nm), and long-wave UV light (365 nm) (Utthamarajan, 1983).

HPTLC

The HPTLC method, derived from TLC, is a modern, sophisticated, and automated separation technique. Pre-coated HPTLC graded plates and an autosampler were used to achieve precision, sensitivity, and significant separation, both qualitatively and quantitatively. HPTLC is a valuable quality assessment tool for efficient and cost-effective assessment of botanical materials. It offers a high degree of selectivity, sensitivity, and rapidity, combined with a single-step sample preparation. Therefore,

it can be conveniently adopted for routine quality control analyses. Additionally, it offers a chromatographic fingerprint of phytochemicals, which are suitable for confirming the identity and purity of Phyto therapeutics (Bladt, 1986).

Chromatogram Development

Chromatogram development was carried out in CAMAG twin-trough chambers. The sample elution was based on the adsorption capabilities of the components to be analyzed. Following elution, plates were removed from the chamber and air dried prior to scanning (Bladt, 1986).

Densitometric scanning

The plates were scanned under ultraviolet (UV) light at 366 nm, and the data were integrated using computer-assisted methodology for analytical gas chromatography (CAMAG) software. Chromatographic fingerprints were generated to identify phytoconstituents present in each sample, and the corresponding Rf values were recorded and tabulated (Bladt, 1986).

Results

Organoleptic Characteristics

Table 2: The organoleptic characteristics of the samples (S1-S4)

Parameter	S1	S2	S3	S4
Sample				
Physical state	Solid	Solid	Solid	Solid
Nature	Coarse powder	Coarse powder	Coarse powder	Coarse powder
Odor	Characteristic	Characteristic	Characteristic	Characteristic
Texture	Rough	Rough	Rough	Rough

Flow Property	Non-free-flowing	Non-free-flowing	Non-free-flowing	Non-free-flowing
Appearance	White crystalline	White crystalline	Pale whitish crystalline	Pale whitish-grey

The organoleptic characteristics of the four samples are presented in Table 2. All samples were solid, coarse powders with a characteristic odor, rough texture, and non-free-flowing properties. Differences were observed in appearance, with S1 and S2 exhibiting a white crystalline appearance, S3 showing a pale whitish crystalline appearance, and S4 exhibiting a pale whitish-grey appearance.

Solubility Profile

Table 3: Solubility/Dispersibility of Samples in Different Solvents (S1- S4)

Solvent	Solubility/Dispersibility			
	S1	S2	S3	S4
Chloroform	Insoluble	Insoluble	Insoluble	Insoluble
Ethanol	Insoluble	Insoluble	Insoluble	Insoluble
Water	Soluble	Soluble	Soluble	Soluble
Ethyl acetate	Insoluble	Insoluble	Insoluble	Insoluble
Dimethyl sulfoxide (DMSO)	Insoluble	Insoluble	Insoluble	Insoluble

All four samples (S1–S4) were soluble in water and insoluble in chloroform, ethanol, ethyl acetate, and DMSO.

Table 4: Physicochemical properties of Samples (S1-S4) (mean ± SD, n = 3)

Parameter	S1	S2	S3	S4
Loss on drying at 105 °C (%)	0.446 ± 0.367	0.246 ± 0.065	0.176 ± 0.083	0.2 ± 0.108
Total ash (%)	92.77 ± 3.27	87.6 ± 2.64	82.57 ± 2.77	91.3 ± 1.044
Acid insoluble ash (%)	0 ± 0	0 ± 0	0 ± 0	0 ± 0
Water soluble extract (%)	0.408 ± 0.178	0.350 ± 0.089	0.257± 0.042	0.517 ± 0.261

Alcohol soluble extract (%)	0.015 ± 0.003	0.011 ± 0.006	0.022 ± 0.003	0.19 0.01

The physicochemical properties of the four samples are presented in Table 4. The loss on drying values ranged from 0.176 ± 0.083% to 0.446 ± 0.367%, with S1 exhibiting the highest moisture content and S3 the lowest. Total ash content varied between 82.57 ± 2.77% and 92.77 ± 3.27%, with the highest value observed in S1 and the lowest in S3. Acid-insoluble ash was not detected in any of the samples.

The water-soluble extractive values ranged from 0.257 ± 0.042% to 0.517 ± 0.261%, with S4 showing the highest water-soluble extractive content. Alcohol-soluble extractive values were comparatively lower, ranging from 0.011 ± 0.006% to 0.190 ± 0.010%, with S4 exhibiting the highest alcohol-soluble extractive value among all samples.

Table 5: Morphological characteristics and particle size distribution of the samples determined by SEM

SEM image	S1	S2	S3	S4
Cluster view	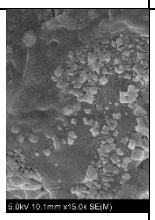	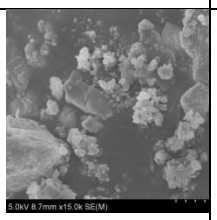	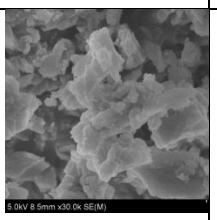	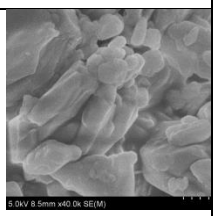
Categorized view	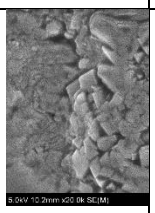 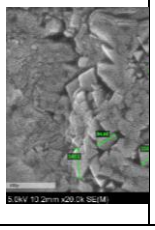	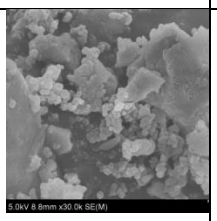 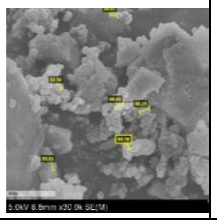	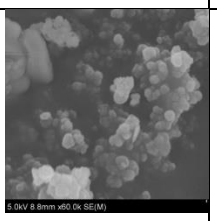 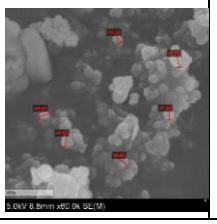	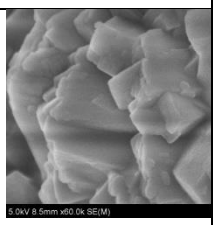 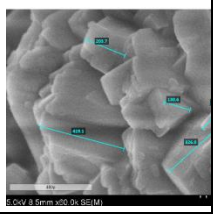

SEM micrographs revealed the presence of clustered particles as well as distinct particle distributions in all four samples. Morphological examination demonstrated noticeable differences in particle size among the samples. The SEM analysis of S1 revealed an average particle size ranging from 64.60 µm–140.1 µm, followed by 33.37–53.01 µm, 43.13–68.76 nm, and 130.6–419.1 nm in S2, S3, and S4, respectively. The SEM analysis indicated a substantial reduction in particle size from the micrometer scale in S1 and S2 to the nanometer scale in S3 and S4. This finding indicates a significant alteration in particle characteristics following processing. The possible effects of frying on particle fragmentation and crystal structure modification should be considered. Nevertheless, the magnitude of the reduction observed requires further validation and mechanistic explanation to establish whether the frying process directly contributes to nanoparticle formation. These variations in the particle size distribution can potentially affect the bioavailability and efficacy of samples.

The observed reduction in particle size may influence physicochemical properties, including surface area and dissolution behavior, which could subsequently affect biological performance. However, further investigations are required to elucidate the mechanisms responsible for the observed particle size changes and to establish their relationship with the processing conditions.

FTIR

FTIR spectroscopy effectively determines the structural features of compounds or atomic interactions between molecules based on the individual energy absorption of specific bonding environments. In S1, there are 3435, 2594, 2323, 2108, 1714, 974, 744, 660, and 485 cm^{-1} peaks (Fig. 1).

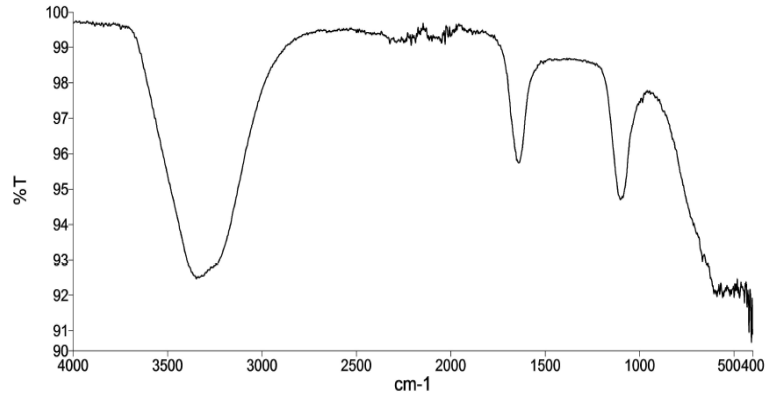

Fig. 1. FTIR spectra of S1

In the S1 spectrum, the presence of a broad absorption peak at 3435 cm^{-1} was assigned to the O-H stretching vibration and exhibited alcohol characteristics. The C=O stretching vibration was observed at 1714 cm^{-1}, and aromatic C-H deformation was observed at 1177 cm^{-1}.

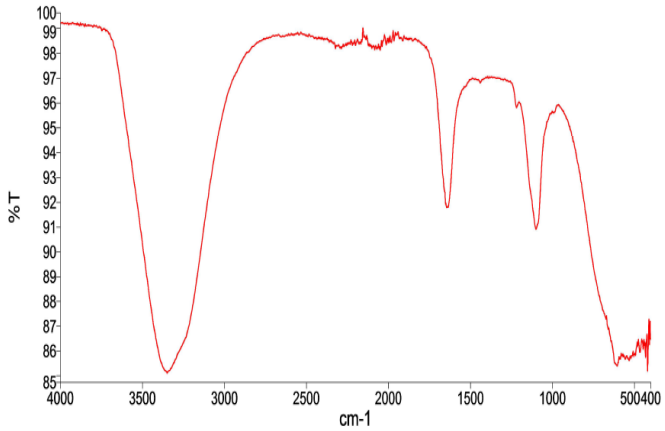

Fig. 1. FTIR spectra of S1

In Figure 2, the aromatic NH2 vibration frequency of a broad peak is observed at 3471 cm-1 in S2 which represents the characteristic of the primary amine and its C=O and -COCN stretching vibrations appearing at 1739 and 1127 cm−1, respectively.

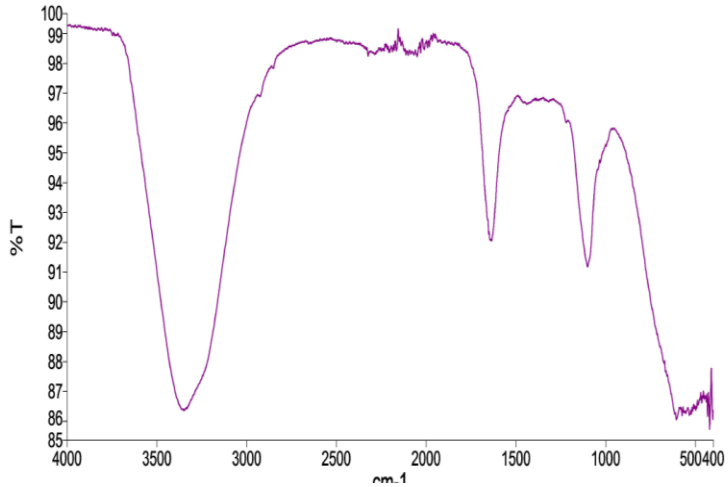

Fig. 3. FTIR spectra of S3

Figure 3 illustrates the FTIR spectrum of S3; the broad absorption peak of the OH and NH2 stretching vibration is observed at 3433 cm−1 and represents the characteristics of alcohol. The O-H deformation vibration has been assigned to 1464 cm−1, and the aromatic O-H deformation and C-O stretching vibration interaction is seen at 1190 cm−1.

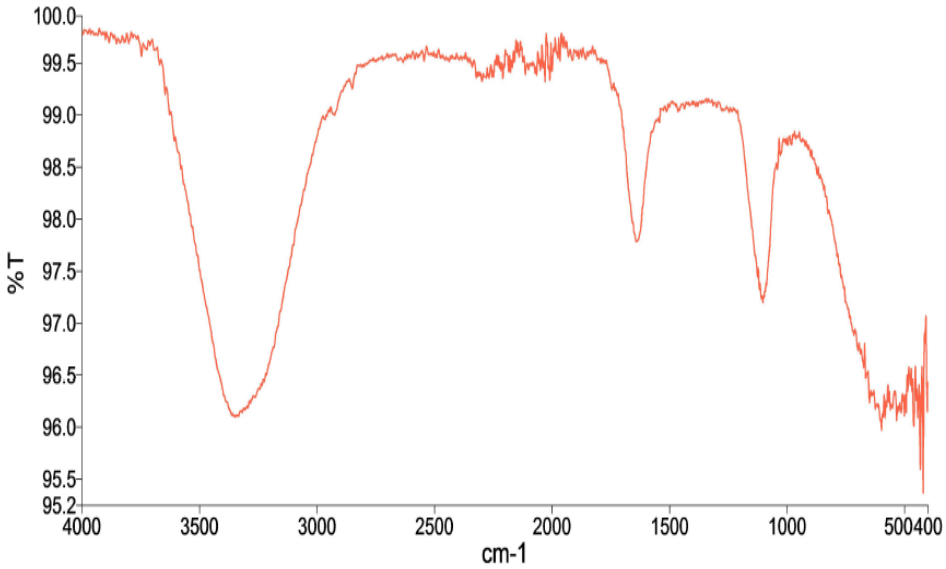

Fig. 4. FTIR spectra of S4

Figure 4 illustrates the FTIR spectrum of S4. The broad absorption peak of the O-H stretching vibration is observed at 3424 cm−1. The C=O stretching vibration is observed at 1672 cm−1, and the aromatic O-H deformation and C-O stretching vibrational interaction are observed at 1162 cm−1.

TLC and HPTLC

Sample 3

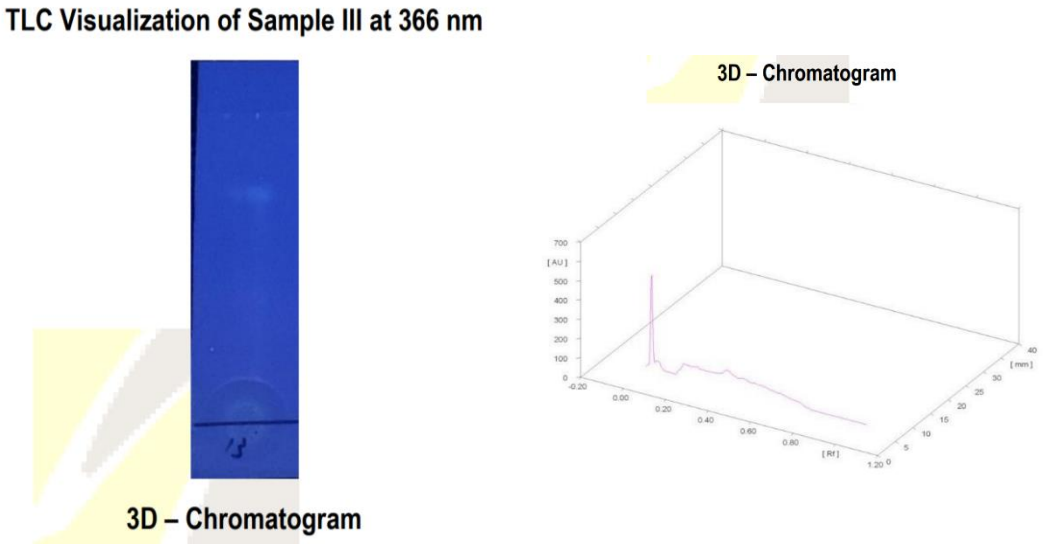

Fig. 5. TLC Visualization of Sample III at 366 nm

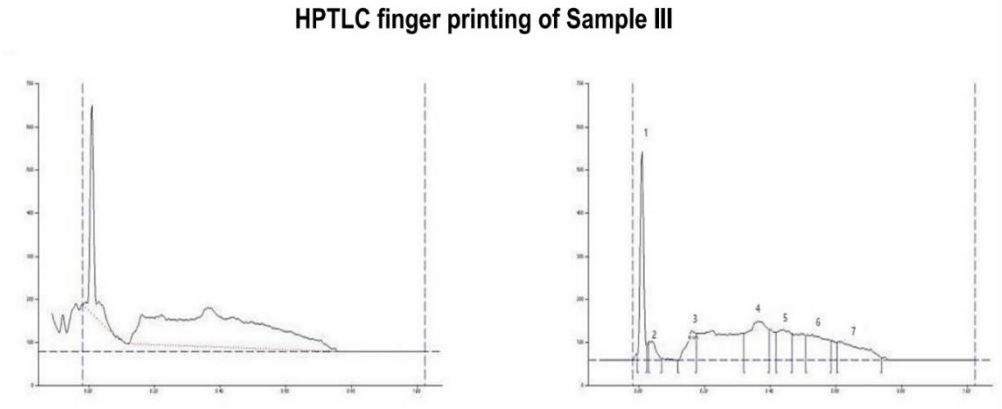

Fig. 6. HPTLC finger printing of Sample III

Peak Table

Peak	Start Rf	Start Height	Max Rf	Max Height	Max %	End Rf	End Height	Area	Area %
1	-0.00	13.3	0.01	483.0	56.19	0.02	32.2	2846.7	21.66
2	0.03	43.1	0.03	43.8	5.10	0.07	3.6	540.2	4.11
3	0.12	0.2	0.16	68.6	7.98	0.18	62.0	1107.3	8.43
4	0.32	62.3	0.37	90.6	10.54	0.40	70.1	3012.2	22.92
5	0.42	65.2	0.44	70.6	8.22	0.47	61.2	1675.1	12.75
6	0.51	57.5	0.53	59.7	6.95	0.59	44.9	2071.9	15.77
7	0.61	42.1	0.62	43.2	5.02	0.74	5.7	1887.9	14.37

Fig. 7. The Peak Table Sample 3

HPTLC fingerprinting analysis of the S3 reveals the presence of six prominent peaks based on the presence of six versatile phytocomponents present in it. The retention factor (Rf) value of the peaks ranges from 0.03– 0.61.

Sample 4

TLC Visualization of Sample IV at 366 nm

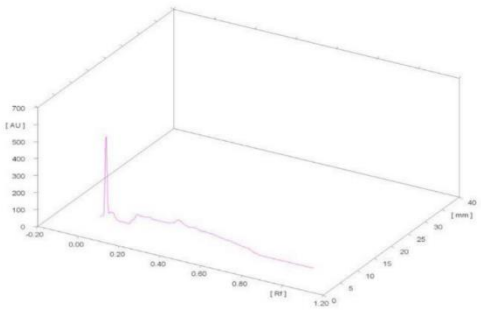

3D – Chromatogram

Fig. 8. TLC Visualization of Sample IV at 366 nm

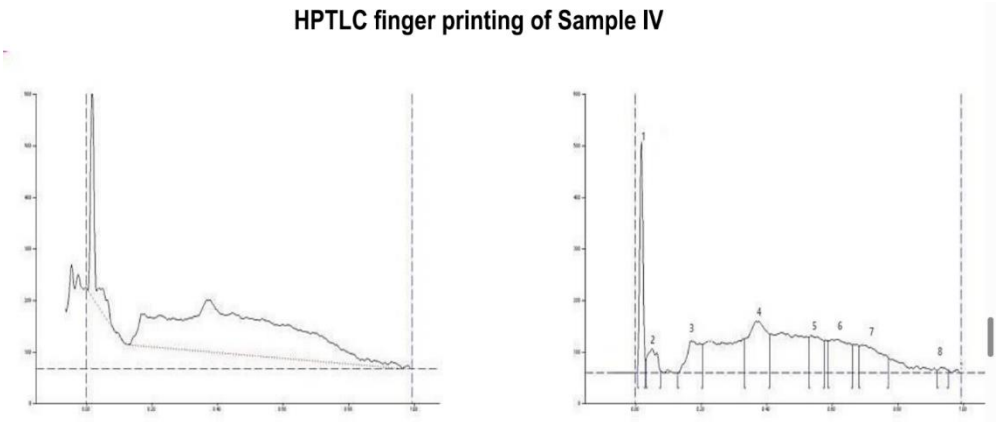

Fig. 9. HPTLC finger printing of Sample IV

Peak Table

Peak	Start Rf	Start Height	Max Rf	Max Height	Max %	End Rf	End Height	Area	Area %
1	0.01	2.2	0.02	447.8	51.97	0.03	23.9	2478.9	17.60
2	0.03	26.0	0.05	47.7	5.54	0.08	3.7	746.7	5.30
3	0.13	0.8	0.18	61.9	7.19	0.21	56.0	1521.1	10.80
4	0.33	66.0	0.38	100.5	11.66	0.41	75.4	3297.6	23.41
5	0.53	68.9	0.54	73.1	8.49	0.58	62.4	1642.6	11.66
6	0.59	62.2	0.61	65.1	7.55	0.66	55.1	2258.2	16.03
7	0.68	51.9	0.69	54.3	6.30	0.77	29.5	1994.8	14.16
8	0.92	4.7	0.93	11.2	1.30	0.96	5.9	147.1	1.04

Fig. 7. The Peak Table Sample 4

HPTLC fingerprinting analysis of the S4 revealed eight prominent peaks based on the presence of eight versatile phytocomponents present in it. The Rf value of the peaks range from 0.01– 0.92.

Discussion

The present study demonstrated that the four samples (S1–S4) possessed similar organoleptic characteristics, including solid coarse powder form, characteristic odor, rough texture, and non-free-flowing nature, indicating consistency in their basic composition. However, slight variations in appearance were observed, suggesting that processing may have influenced the physical characteristics of the samples. The solubility profile showed that all samples were soluble in water and insoluble in organic solvents, indicating the predominance of polar constituents and supporting their potential for aqueous absorption.

Physicochemical analysis revealed low moisture content in all samples, which is favorable for product stability and shelf life. The high total ash values indicate a substantial mineral content, while the absence of acid-insoluble ash suggests freedom from siliceous impurities and good processing quality. The higher water-soluble extractive values compared to alcohol-soluble extractives further support the predominance of water-soluble constituents.

SEM analysis demonstrated marked differences in particle size distribution among the samples. S1 and S2 contained particles in the micrometer range, whereas S3 and S4 exhibited particles in the nanometer range, indicating significant particle size reduction following processing. Such reduction may enhance surface area, dissolution, and bioavailability. FTIR analysis identified common functional groups, including hydroxyl, amino, and carbonyl groups, across all samples, while minor shifts in absorption peaks suggest possible structural modifications resulting from processing.

HPTLC fingerprinting revealed six major peaks in S3 and eight peaks in S4, indicating differences in phytochemical composition between the samples. The greater number of peaks observed in S4 suggests the presence of additional phytoconstituents or processing-induced chemical changes. Overall, the findings indicate that processing influences the physicochemical, morphological, and phytochemical characteristics of the samples, which may ultimately affect their therapeutic performance. Further studies are required to establish the relationship between these changes and biological activity.

Conclusion

These results indicated that all four samples exhibited similar properties. Samples S1 & S2, S3, and S4 appear white crystalline, pale white crystalline, and pale whitish-grey, respectively. All the samples were dissolved in water. FTIR spectroscopy is valuable for determining the structural features of compounds and their bonding environments. In S1, a broad absorption peak is assigned to the O-H stretching vibration, indicating alcohol characteristics. In S2, an aromatic NH2 vibration frequency is observed, indicating primary amine characteristics. These are more likely from tiny impurities or water, not the main part of the salt. In S3, a broad absorption peak is observed for alcohol characteristics, whereas in S4, a broad absorption peak is observed for the O-H stretching vibrations. The presence of hydroxyl (O–H) functional groups observed in FTIR analysis of plant-based preparations may correspond to phenolic and flavonoid compounds derived from these plants. The HPTLC fingerprinting analysis of S3 and S4 revealed six and eight prominent peaks, respectively, indicating the presence of versatile phytocomponents. The combination of spectroscopic and chromatographic techniques facilitated a comprehensive understanding of the chemical composition of the samples. The SEM analysis of S1 revealed an average particle size ranging from 64.60–140.1 μm, followed by 33.37–53.01 μm, 43.13–68.76 nm, and 130.6–419.1 nm in S2, S3, and S4, respectively. The formation of nano-sized salt particles may increase the surface area and dissolution rate of the salt, enhancing saltiness perception. Consequently, a lower quantity of salt may be required to achieve the desired taste, potentially reducing overall sodium intake. Since excessive sodium consumption is a major risk factor for hypertension, the use of nano-sized salt particles may indirectly contribute to blood pressure control. However, further studies are needed to confirm this mechanism and its clinical relevance. Further analyses may offer valuable insights into the specific pharmacological actions of these compounds.

References

India Pharmacopeia I Volume I, Government of India, Ministry of Health and Family welfare, Indian Pharmacopeia commission, 2014.

Komsta L, Waksmundzka-Hajnos M, Sherma J. Thin layer chromatography in drug analysis. CRC Press, Taylor and Francis; 2013.

Murugesha muthaliyar KS. Gunapadam-Muligai vakuppu, Materia Medica part I & II. 1st ed. Government press; 1936.

Pharmacopoeial Laboratory for Indian Medicine (PLIM) Guideline for standardization and evaluation of Indian medicine which include drugs of Ayurveda, Unani and Siddha systems. Department AYUSH. Ministry of Health and Family Welfare, Govt. of India.

Sambasivam Pillai TV. Tamil – English Dictionary Vol I and V. Madras: Government of Tamil nadu; 1994.

Thiyagarajan R. Gunapadam Thadhu jeeva vagupu part II&III. Chennai: Dept of Indian Medicine and Homeopathy; 2006.

Uththamarajan KS. Siddha maruthuvanga surukkam. 6th ed. Chennai: Dept of Indian Medicine & Homeopathy; 1983.

Wagner H, Bladt S. Plant drug analysis: a thin layer chromatography atlas. 2nd ed. Springer-Verlag Belgium: Heidelberg; 1996.